Numerical Methods in Civil Engineering, 6-3 (2022) 51-63

Numerical Methods in Civil Engineering

Journal Homepage: https://nmce.kntu.ac.ir/

Seismic Performance of seat-type bridges with elastomeric bearings

Mohammad Barkhordari* **and Saeed Tariverdilo****

ARTICLE INFO

RESEARCH PAPER

Article history:
Received:
June 2021.
Revised:
August 2021.
Accepted:
October 2021.

Keywords:
seat-type bridge, elastomeric bearing, shear key, coefficient of friction, unseating.

Abstract:

In Iran and some other countries, elastomer bearings in seat-type bridges are used with no sole/masonry plates and there is no positive connection between superstructure and substructure. Different codes have diverse provisions regarding the coefficient of friction (μ) between elastomer bearing and superstructure/substructure and also the design strength of shear keys (V_{sk}). Developing a finite element model for bearing slip, this paper investigates how different assumptions for μ and V_{sk} could affect the seismic performance. Incremental dynamic analysis is used to investigate the probability of unseating, residual displacement and nonlinear deformation in the substructure on a prototype three-span bridge. While performance during past earthquakes is fairly good, evaluating response using codes' recommended value, i.e., μ=0.2, leads to an unacceptably high probability of unseating. Regarding design strength of shear keys, it is shown that design for weak shear keys could lead to relatively large transverse displacement during small to large earthquakes, and on the other hand, strong shear keys does not provide better protection against large transverse displacement during intense ground shakings.

1. Introduction

Now, it is more than 60 years that reinforced neoprene or natural rubber bearings are used as bearing pads in bridges, where they provide an economic alternative. The main desired feature of the elastomeric bearings is their large vertical stiffness and load-bearing capacity and at the same time, their relatively low horizontal stiffness.

Evidence of "walkout" of elastomeric bearing due to thermal loading triggered infield and laboratory researches to find possible causes and put into question the possibility of the use of elastomeric bearings without endplates. Infield measurements revealed that this problem is pertinent to natural rubber bearings, where paraffin wax is used on the exterior surface of the bearing [1] to provide ozone protection. This leads to a reduced coefficient of friction (μ) and consequently "walkout" of bearing in-service condition due to thermal loading. The use of neoprene, which has much better ozone resistance without the need for protective wax, together with the proper design of the bearing, removes the possibility of "walkout" at service condition. However, there are reported cases of "walkout" at severe earthquake ground motions [2].

* *Ph.D. Candidate, Department of Civil Engineering, Urmia University, Urmia Iran.*

** *Corresponding author: Professor, Department of Civil Engineering, Urmia University, Urmia Iran, Email: s.tariverdilo@urmia.ac.ir*

While conventional elastomeric bearings provide a low-cost option for control of shrinkage and thermal loadings, they also provide a low-tech option for base isolation of bridges. Kelly and Konstantinidis [3] propose the use of unbonded elastomeric bearings without endplates (sole and masonry plates) as an affordable isolator for the developing world. Lack of endplates prevents the development of tensile stress in the elastomeric bearing in the case of relative lateral displacement between superstructure and substructure. For large lateral displacements, slipping rather than shear distortion composes the main component of deflection. Considering that a large number of bridges throughout the world were constructed employing these types of bearings, accounting for slipping of bearing could have a significant impact on the retrofit and renovation cost of existing bridges. Kelly and Konstantinidis also found that unbonded elastomeric bearings could experience shearing strains as large as 200% without any appreciable tearing or cracking. Following extensive experimental and numerical investigations (e.g. [4-6]) on seismic performance of elastomeric bearings, IDOT [7] has introduced a three-tier seismic design strategy including, 1) fusing action of connection force (side retainers and

dowels), 2) providing adequate seat width to avoid unseating, 3) utilizing plastic hinging of elements as the last resort to dissipate earthquake energy.

Maghsoudi-Barmi and Khaloo experimentally investigated the hysteretic response of unbounded elastomeric bearings accounting for long-term application of vertical loading, degradation due to repeated shear loading and post-earthquake service response [8]. They found that although there are changes in the mechanical properties of the elastomeric bearings, still they could provide satisfactory performance. Maghsoudi-Barmi et al., using incremental dynamic analyses and adopting bilinear modeling for unbounded elastomeric bearing investigated the seismic performance of three-span bridge [9]. They found significant improvement in the seismic response of the bridge when accounting for the bearing slip.

While friction mainly controls the response of unbonded elastomeric bearings, there is a wide range of variation for μ as proposed by different codes/researchers/institutes. Schrage [10] reported that μ is inversely proportional to compressive stress, which was verified experimentally by Konstantinidis, et al. [11] and later by Steelman et al. [4]. Steelman et al. applying quasi-static loading with increasing strain rates reported a wide range of variation in μ for compressive stresses ranging from 1 to 6 MPa. For example, for compressive stress of about 2.6 MPa, measured μ, varies between 0.26 to 0.37. Filipov et al. [12] used kinematic μ of 0.45 to 0.5, in their numerical simulations evaluating seismic performance of seat-type bridges. Huang, Liu and Ding [13] comparing results of experimental works on the frictional response of elastomeric bearing with their stick-slip model, reported a μ value of about 0.5 to 0.6 between elastomeric bearing and concrete contact surface.

Different codes'/institutes' provisions regarding connection design force (design force for shear keys/side retainers/dowels) and proposed μ value are summarized in Table 1. By thorough review of this table, different approaches could be summarized as follows

- There is no consensus on the value of coefficient of friction. Different codes adopt different values for μ ranging from 0.1 up to 0.4. Also, there is ambiguity regarding the required controls on the shear deformation of the elastomeric bearings.
- The case of unbounded elastomeric bearings is not covered.
- Different codes adopted completely different approaches regarding the need for positive connection between the superstructure and substructure and the required design force.

Table. 1: Treatment of connection force and friction by different institutes/researchers

Institute	**Proposal regarding connection of elastomeric bearing and lateral force transfer mechanism and design value**
AASHTO/NSBA [14]	• Elastomeric bearing with sole plate and without masonry plate (connected only to superstructure) • Requires no positive connection between superstructure and substructure • Lateral force transfer is allowed to be done by friction with μ of 0.2
AASHTO [15]	• Allows slipping in elastomeric bearing in the event of large earthquakes (14.6.5.2) • Elastomeric bearing could be a designed sacrificial element to reduce seismic demand on substructure
AASHTO Seismic [16]	• The emphasis is on bridges with integral cap beams and seat-type abutments • Sacrificial elastomeric bearings whose connections have failed, and upon which the superstructure is slipping, are allowed in abutments • Requires connection design force only for regions with low seismicity and only in the restrained bearings • For regions with moderate to high seismicity, there is no provision for connection design force
FHWA [2]	• Evaluation of bridge vulnerability requires positive connection of superstructure and substructure • In this evaluation it is generally assumed that connections are futile failed
Caltrans [17]	• The emphasis is on bridges with integral cap beams and seat-type abutments • Elastomer bearing is considered as a sacrificial element • Dynamic coefficient of friction is assumed to be 0.40 and 0.35 between elastomer and concrete/steel • Shear strain in the elastomer bearing is limited to 1.5 • Shear key design force is determined considering slipping of the abutment foundation (spread footing)
IDOT [7]	• In IDOT type I bearing, elastomer bearing has only a sole plate and directly bears on the substructure concrete (similar to AASHTO/NSBA proposed bearing) • Nominal connection design force for dowels of fixed bearings and also for side retainers is assumed to be 20% of superstructure tributary dead load
FHWA-ICT-18-013 [6]	• Proposes design of retainers for 90% of the superstructure dead load to limit slip and avoid unseating
Chinese Guidelines for Seismic Design of Highway Bridges [18]	• Dynamic coefficient of friction between elastomer and concrete/steel is assumed to be 0.15/0.10 • Does not allow sacrificial bearings

Wang et al. [19] investigated statistical characteristics of μ using molecular dynamic simulations. They found that the distribution of frictional force could be approximated by a normal distribution. They also found that the mean value of atomic friction force rises linearly by the normal pressure, which is opposed to the findings of Schrage. The normal distribution of friction force is also in agreement with experimental findings of Chang *et al.* [20].

Omrani et al. [21] investigated the effect of epistemic uncertainty on the performance of two spans bridge with seat-type abutment and integral bent cap. They found strong interaction between the assumed response models for backfill and shear keys in bridges with moderate to high skew angles. This is mainly due to the well-known interaction between shear keys transverse force at cute corners of abutment and backfill's longitudinal force (Kawashima et al. [22] and Song et al. [23]). To reduce this interaction, Wu suggests using a larger gap in abutment expansion joints. Filipov et al. [5] recommended an increase in the design force of the retainers to avoid unseating in skew bridges. This shows how assumptions regarding the design force of shear keys/side retainers could affect the seismic performance of bridges.

Seat-type bridges are used in different countries with different details regarding the end plates (masonry and sole plates) of elastomeric bearings and connection of the superstructure to substructures, which is briefly reviewed in Table 1. In Iran, elastomeric bearings without masonry and sole plate are widely used. Lack of masonry and sole plate makes the installation process easier and increases admissible construction tolerances. These bridges without positive connection between superstructure and substructure performed very well during Manjil-Rudbar 1990 earthquake (Moinfar and Naderzadeh [24]) and Bam 2003 earthquake (Eshghi and Ahari [25]). In these earthquakes, although there were widespread damages to building structures, damages to bridges near the earthquake center included minor spalling of concrete in the deck due to ponding at expansion joints and also movement in the abutment wall. It seems that same type of construction is also widely in use in China and at least in Wenchuan 2008 earthquake, this detailing resulted in good performance of bridge structures (Kawashima et al. [22]).

There are large variations regarding the proposed coefficient of friction by different codes. Also, there is no consensus with different authorities regarding the connection between superstructure and substructure and its required design force. On the other hand, there are a large number of bridges with unbounded elastomeric bearings in Iran and other countries, where their seismic performance could be crucial in post-earthquake management of the response and recovery. Considering possible variation in the coefficient of friction and shear key design force, this paper investigates the seismic performance of bridges with elastomeric bearing in abutment and also in the piers. Engineering demand parameters of interest include the probability of unseating, residual displacement and plastic deformation in the substructure. Elastomeric bearings considered in this study do not have endplates and also there is no positive connection between superstructure and substructure. The lateral force transfer is accomplished by friction between elastomeric bearing and concrete substructure and at later stage by shear keys. Accounting for a large variation in the improvised μ by different codes/institutes, this paper evaluates the sensitivity of the seismic performance of the bridge to the assumed distribution of μ. This study also considers the effect of different assumptions regarding connection design force (shear keys design strength) on the seismic response of bridges. In the following, after introducing the model bridge, assumptions used in the finite element modeling of different elements are introduced, then ground motions used in the analyses and the procedure used for incremental dynamic analysis is given, and finally results obtained from the study are presented.

2. Prototype Bridge

The model bridge is a 50 m long, three spans (15/20/15 m) continuous superstructure with a width of 12 m (Figure 1). This is a hypothetical bridge with dimensions simulating a typical three-span bridge. The bridge is located in Tehran and designed according to the requirements of publication number 463 that covers the seismic design of bridges in Iran [26]. The bents are two piers concrete frames, and the superstructure consists of I shape steel girders with a 200 mm thick concrete deck and a 50 mm overlaying asphalt. The elastomeric bearings are designed following AASHTO guidelines [15] and only considering non-seismic loads.

Design spectral acceleration at the fundamental period of the bridge (about 0.86 sec for both longitudinal and transverse directions) is 0.56g. The dimension of elastomeric bearings in abutments and bents are 300x300x100 mm, with no masonry or sole plates. No dowels are used to connect the deck to the column cap. Expansion joint width between deck and abutment back wall is assumed to be 50 mm. Total deck height, from top of bearings to top of concrete deck is 1700 mm. Shear keys are located on the bents and also on the abutments. The model assumes rigid foundation. Some of design parameters are given in Table 2.

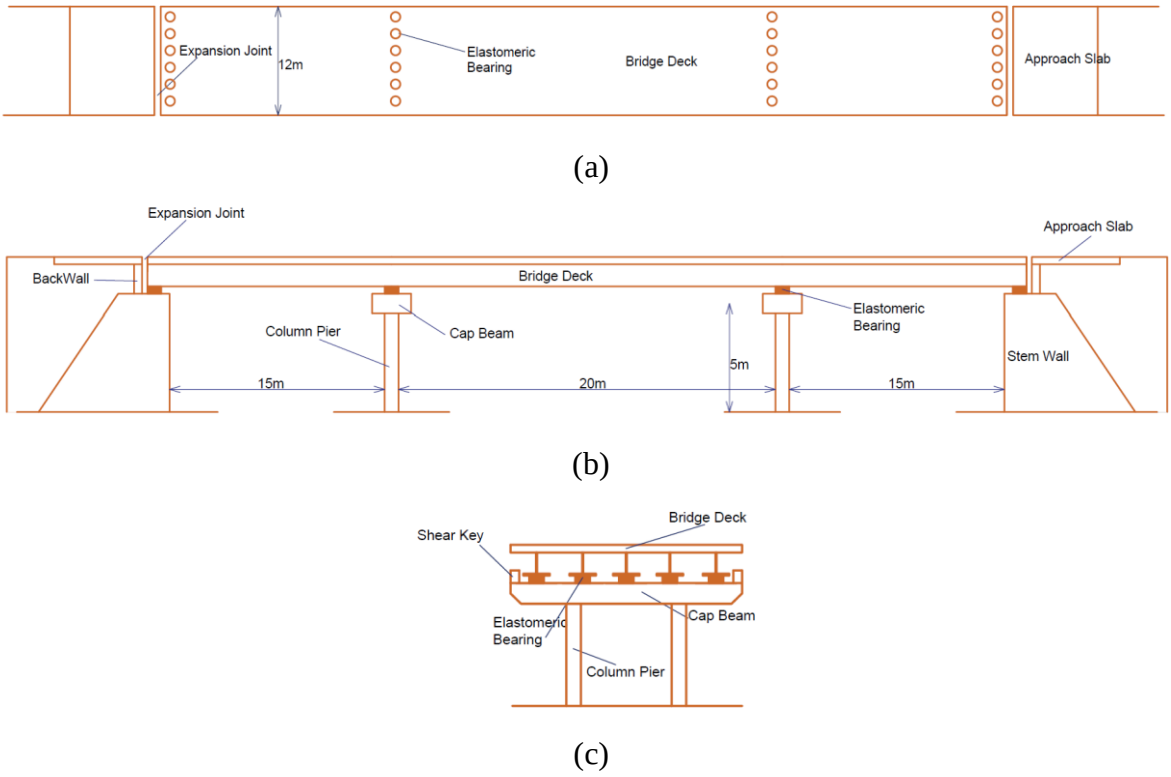

Fig. 1: The model bridge, a) plan, b) longitudinal view, c) bent transverse section.

Table. 2: Design parameters of the model bridge

Materials/Elements	**Dimension/Properties**		
Concrete	$f_c^{'}$=40 MPa		
Rebars	Yield stress 400 MPa, Ultimate Strength 500 MPa		
Column	Diameter: 1200 mm Height: 5000 mm	Longitudinal bars: 30T28 (rebar dia.=28 mm)	Transverse Spirals: T14 @ 75 mm
Cap Beam	Height: 1200 mm Width: 1500 mm	$I_x = 0.216\ m^4$	$I_y = 0.337\ m^4$
Abutment Back Wall	Width: 12000 mm Height: 1700 mm Thickness: 150 mm	Longitudinal bars: T16 @ 300mm	Transverse bars: T16 @ 300mm
Elastomeric Bearing	Length: 300 mm Width: 300 mm Height: 100 mm	Elastomer: 8 layers Layer thickness : 10 mm	Steel Shims: 7 layers Layer thickness: 3 mm

3. Finite Element Modeling

This research employs OpenSees [27] for finite element analysis of the prototype model bridge. Different material and element types in the library of the OpenSees are used for this purpose as will be discussed in this section.

Modeling of elastomeric bearing frictional and distortional response is performed using a combined OpenSees element. This element combines a zero-length flatSliderBearing element modeling Coulomb friction, with a combination of elastomericBearingBoucWen, axialSP, and elastic stiffnesses to model distortional/axial/rotational responses of the elastomeric bearing, as is depicted in Figure 2a. Before the onset of slip, nonlinear distortional response due to the use of the Bouc-Wen model for the elastomeric bearing is evident in the response of the combined element in Figure 2b.

The finite element model of the elastomeric bearings does not account for possible uplift force on the bearings. However, control of the vertical forces on the bearings in all stages of the analyses confirmed that the net vertical force on the bearing is downward.

The column elements have been modeled using nonlinearBeamColumn element that is a forced-based element modeling nonlinear deformation through distributed plasticity. Five Gauss points are used in each element with two points at elements endpoints (employing Gauss-Lobatto integration scheme). Each section of the column is modeled using fiber sections with discretization including 6 radial and 24 circumferential divisions. Steel rebars are modeled using Hysteretic material property that is modified to account for longitudinal bar buckling ([28-30]) and low cycle fatigue using Fatigue material. Rainflow cycle counter is used by OpenSees to evaluate the accumulation of damage using the Coffin-Manson relationship. For modeling concrete confinement, modified

Mander model [31] is adopted. Typical hysteretic response of the steel rebars and confined concrete is given in Figures 2c and 2d, where expected strength of materials is used in the simulations. Considering that cap beams are capacity protected element, they are modeled using elasticBeamColumn element with section properties given in Table 1.

Although employing results of experimental programs [32], CALTRANS includes requirements for the design of ductile shear keys, as most of the shear keys in the existing bridges do not satisfy these requirements and has brittle failure. Therefore, the simulated response of shear keys is modeled by a gap followed by a linear model and then by a steep softening. This is done using a twoNodeLink in the OpenSees element library that is composed of ElasticPPGap (elastic perfectly plastic gap uniaxialMaterial) in series with ENT (elastic no tension uniaxialMaterial). Figure 2e gives a typical cyclic response of the combined element used in this study to simulate the shear key response.

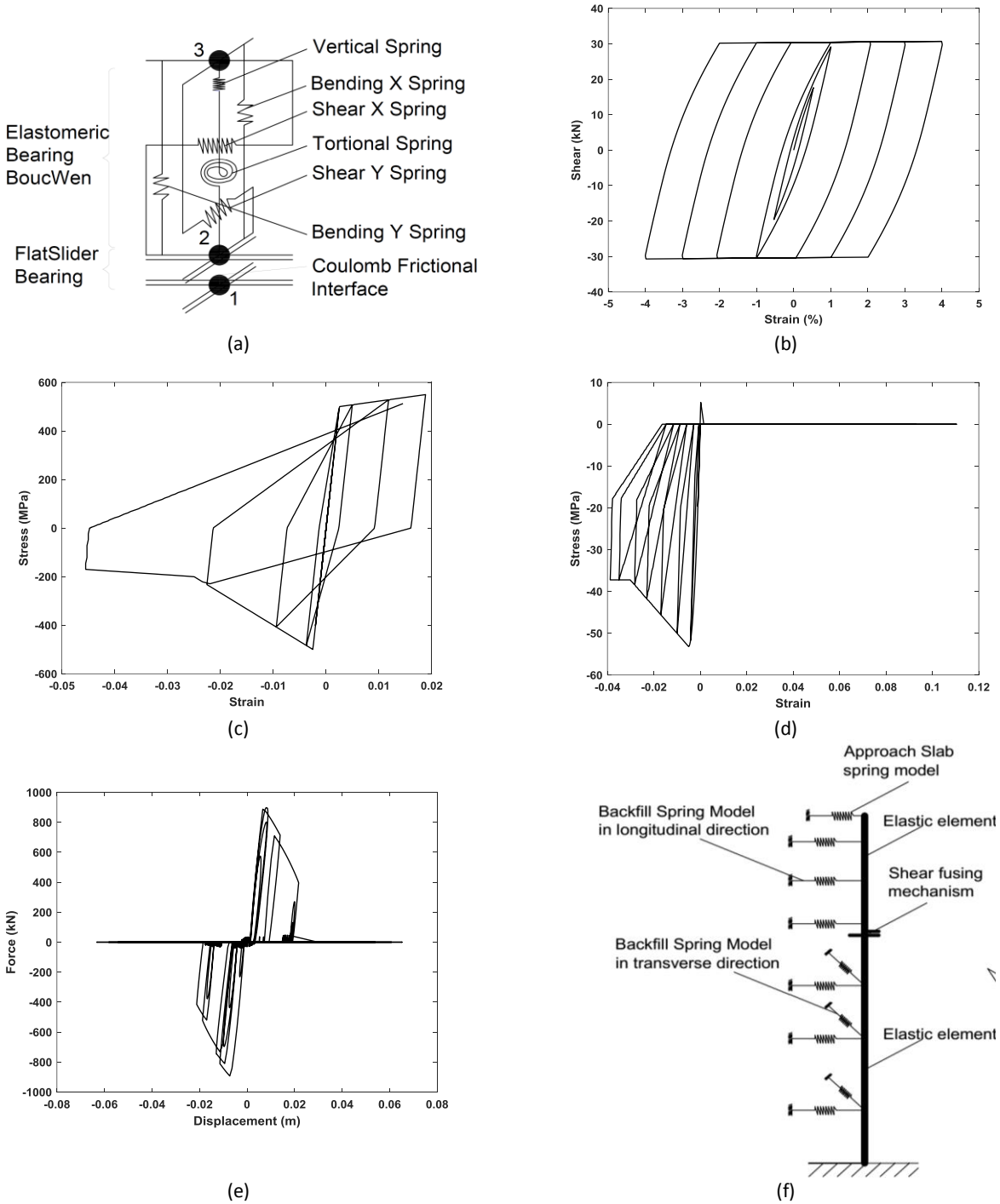

Fig. 2. Simulating different element, a) combined element used for modeling elastomeric bearings, b) frictional/distortional response of the combined element for elastomeric bearing, c) simulated cyclic response of rebar, d) simulated cyclic response of confined concrete, e) simulated cyclic response of the combined element for shear key, f) simulation of backwall and backfill

Large longitudinal displacement of deck could result in shear failure of the back wall and mobilization of passive resistance of the backfill (Figure 2d). This could have a significant impact on the seismic performance of the bridge, especially those of short to medium-length bridges. Back walls similar to shear keys are considered sacrificial elements, and like shear keys their seismic response is brittle. The back wall and stem wall are modeled using elasticBeamColumn element and connection of the back wall to the stem wall is modeled using the zero-length element with brittle shear failure implementing ElasticPPGap uniaxial Material. Backfill passive response is modeled implementing twoNodeLink element with a uniaxial material property of QzSimple1 simulating the soil passive response. The strength of the backfill is evaluated using the approach proposed by CALTRANS.

There are two common approaches for modeling ponding which include a contact element (force-based) and a stereomechanical approach (time-based) [33]. Contact element includes a spring with high stiffness in conjunction with a damping element. This study uses OpenSees impactMaterial that is based on Hertz law in conjunction with a nonlinear hysteresis damper.

4. Ground Motions and Incremental Dynamic Analyses

Evaluation of the seismic response of the model bridge is done using incremental dynamic analysis (IDA). This analysis method provides a comprehensive platform for assessing the bridge seismic performance for growing ground motion intensities. Table 3 gives list of ground motions (ground motions) considered in the IDA. Record to record variation could have a significant impact on the bridge performance and its adequacy assessment. To reduce bias in the assessment due to record-to-record variation of ground motions, selection of ground motions is done accounting for magnitude, soil class and fault type epicenter. Selected earthquake ground motion records include 20 records on soil class D of AASHTO (Vs30 between 183 to 366 m/s) and magnitude between 6.5 to 7.5. The strike slip fault with epicenter distance between 10 km and 30 km is considered. PEER ground motion Database Machine (https://ngawest2.berkeley.edu) is employed to select earthquake time series records.

The mean of the selected ground motions is adjusted using the least square method to fit the target spectrum that is a design spectrum with 1000 yrs return period. Then for IDA, records scaled up and down adopting single scale factors of 0.25 to 1.75 in steps of 0.125. Now, different scale factors could be attributed to different ground motion levels, e.g., scale factors of 0.5, 1 and 1.25 could approximately represent hazards with return periods of 100 (Service Level Earthquake (SLE)), 1000 (Design-Basis Earthquake (DBE)) and 2500 yrs (Maximum Considered Earthquake (MCE)).

Table. 3: List of ground motion records considered in incremental dynamic analyses.

Num.	Earthquake/Station	Year	Magnitude	R_{jb} (km)
1	Northern Calif-03/ Ferndale City Hall	1954	6.50	24.69
2	San Fernando/ LA - Hollywood Stor FF	1978	6.61	29.8
3	Tabas, Iran/ Boshrooyeh	1981	7.35	24.25
4	Imperial Valley-06/ Calexico Fire Station	1979	6.53	19.97
5	Corinth, Greece/ Corinth	1987	6.60	25
6	Superstition Hills-02/ Calipatria Fire Station	1989	6.54	17.16
7	Loma Prieta/ Agnews State Hospital	1992	6.93	24.77
8	Landers/ Coolwater	2004	7.28	23.46
9	Niigata, Japan/ NIG022	2007	6.63	25.55
10	Chuetsu-oki, Japan/ Joetsu City	2008	6.68	19.08
11	Imperial Valley-06/ Calipatria Fire Station	1979	6.53	23.17
12	Imperial Valley-06/ Compuertas	1979	6.53	13.52
13	Superstition Hills-02/ El Centro Imp. Co. Cent	1987	6.54	18.2
14	Landers/ Desert Hot Springs	1992	7.28	21.78
15	Landers/ Mission Creek Fault	1992	7.28	26.96
16	Kobe, Japan/ Abeno	1995	6.9	24.85
17	El Mayor-Cucapah, Mexico/ Chihuahua	2010	7.2	18.21
18	El Mayor-Cucapah, Mexico/ Michoacan de Ocampo	2010	7.2	13.21
19	Darfield, New Zealand/ Canterbury Aero Club	2010	7	14.48
20	Darfield, New Zealand/ Christchurch Hospital	2010	7	18.4

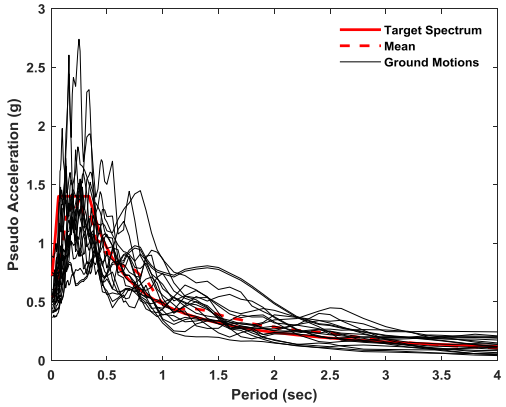

Fig. 3: Spectrum of the selected ground motion compared with target and mean spectrum

5. Results

Evaluation of the seismic performance is done for different strength of shear keys (V_{sk}) and also for different values of μ including 0.20, 0.40, 0.60 and 0.80. Considering the fundamental period of vibration of the bridge in the transverse direction, shear key strength, V_{sk}, is designed for spectral acceleration corresponding to design earthquakes of 100 (SLE), 1000 (DBE) and 2500 yrs (MCE) return periods. Two types of analyses are done, analyses accounting for slipping bearing (modeling the actual response of the elastomeric bearings) and another set of analyses considering nonslip bearings, which ignores possible slip in the bearing. It should be noted that nonslip model has widespread use among engineering community.

Figure 4 compares the deck displacement for models of slipping bearing (μ=0.4) and nonslip bearing for Cape Mendocino ground motion with a scale factor of 1.5. While the nonslip model (that is commonly used in performance assessment) shows no residual displacement, in the model accounting for bearing slip, there is significant residual displacement in both longitudinal and transverse directions. In addition to significant residual displacement, slipping also leads to large increase in the maximum displacement. These show importance of modeling of bearing slip in any assessment of bridges with elastomeric bearings.

The significant difference observed between the results of nonslip and slipping bearing in Figure 4 which is in odds with AASHTO and FHWA provision regarding minimum seating width that is independent from bearing type and kind of connection between superstructure and substructure.

Figure 5 shows the effect of an increase in the intensity of ground motion on the deck displacement. The figure shows deck displacement for Landers ground motion with scale factors of 1.00 and 1.75 for the model with slipping bearings (μ=0.4). As could be seen, an increase in the ground motion intensity results in a significant increase in the deck displacement. Figure 6 depicts the evolution of deck displacement for increasing scale factors in IDA for slipping (μ=0.4) and nonslip models. The figure also gives the mean and extreme values of the response parameter for increasing IDA. Slipping leads to a significant increase in the mean and variation of the deck displacement.

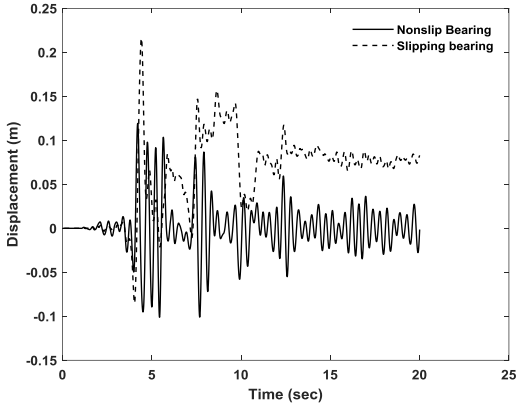

(a)

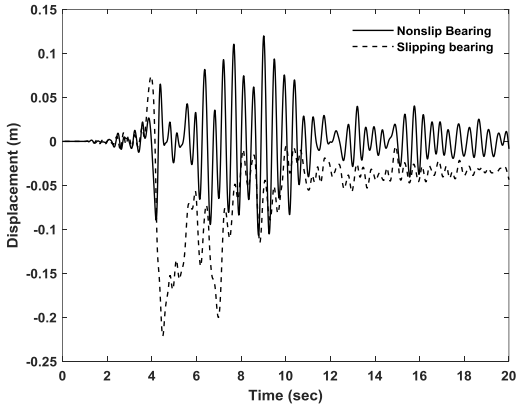

(b)

Fig. 4: Deck displacement of models slipping bearing (μ=0.4) and nonslip bearing for Cape Mendocino ground motion, a) longitudinal direction, b) transverse direction

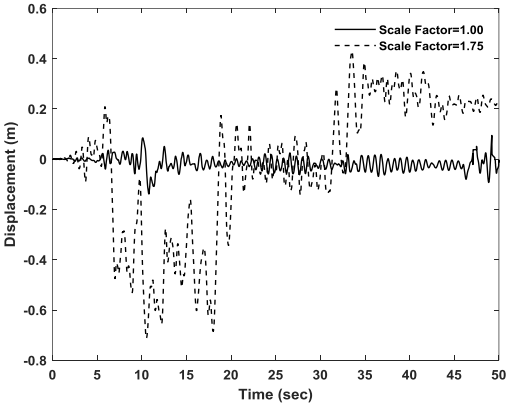

Fig. 5: Deck displacement for Landers ground motion scaled by scales 1.00 and 1.75 for slipping bearing (μ=0.4)

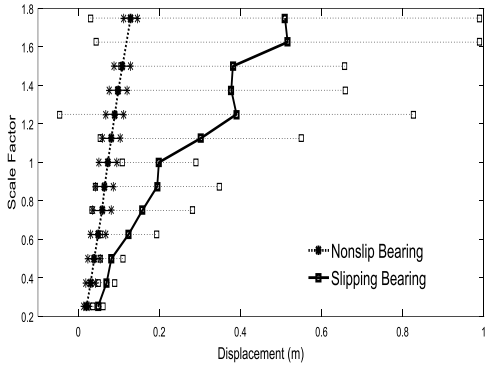

(a)

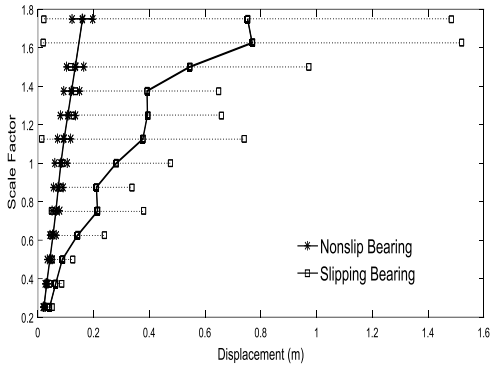

(b)

Fig. 6: Evolution of deck displacement for increasing scale factors in slipping (μ=0.4) and nonslip models, including mean, mean plus and minus standard deviation, a) longitudinal direction, b) transverse direction

Longitudinal response

Considering the possible variation in μ, Figure 7 shows the effect of μ on the deck displacement for increasing intensity of ground motions. A substantial change in displacement due to change in μ is apparent in the figure and this could completely change any judgement on the adequacy of the design seating width. Considering the distribution of displacement (mean/min/max) at each intensity, the probability density function of displacement is approximated by a lognormal distribution. It should be noted that the recommended coefficient of friction by AASHTO and Chinese code for seismic design of highways is 0.2 and 0.15, respectively. For these values of μ, unacceptably very large displacements are evident in Figure 7a. Design seating width in these figures is calculated using FHWA [2] formulae that is slightly larger than that by AASHTO.

A sudden increase or decrease in the displacement could be observed for the maximum response in the cases of μ=0.2 and 0.4. No such changes are seen for the mean and minimum responses. That is an indication of the dynamic instability of the bridge due to slipping. No such behavior is observed for the coefficient of friction of 0.6 and 0.8, as larger damping of the sliding system prevents this type of instability.

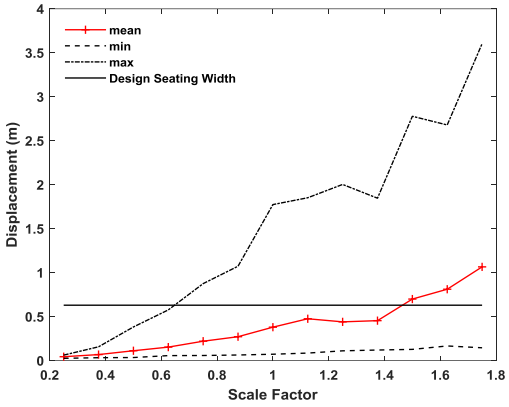

(a)

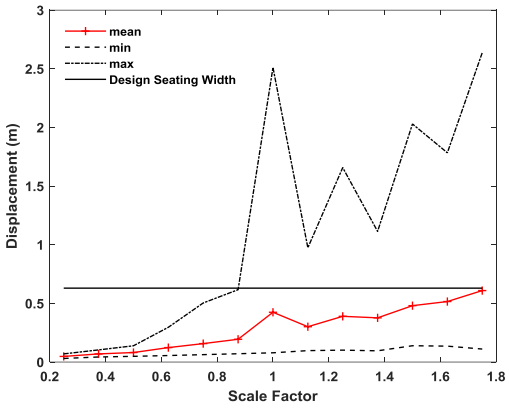

(b)

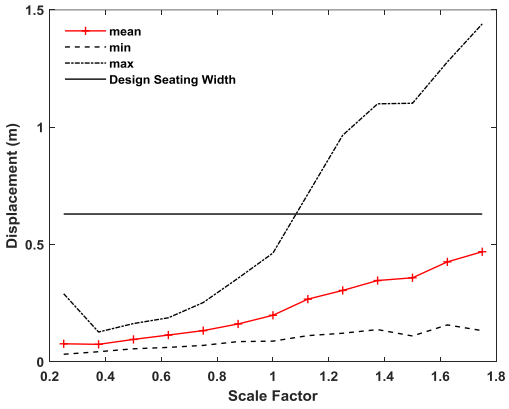

(c)

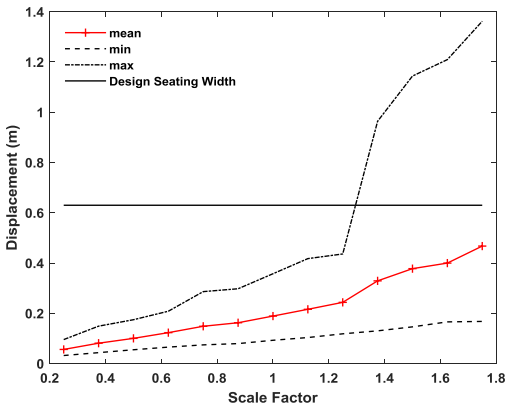

(d)

Fig. 7: Deck displacement for increasing intensity of ground motions, a) μ=0.2, b) μ=0.4, c) μ=0.6, d) μ=0.8

Now assuming a normal distribution function f for μ, the probability of unseating (P) could be evaluated as follows

$$P(\text{unseating}) = \sum_{i=1}^{n} P(\text{unseating}|\mu = \mu_i) f(\mu = \mu_i) \quad (1)$$

It should be noted that both AASHTO and FHWA considering the devastating effect of unseating, evaluate risk of unseating for MCE level ground motion intensity, rather than DBE level that is commonly used for design of other components. Therefore, in the following analyses unseating probability at MCE level ground shaking is of main concern, and spectral acceleration at this level can be approximated by 1.25 times that of SDB. Noting that there is no consensus among different authorities regarding the value of μ, calculation of failure probability is done for two cases. In the first case, with constant standard deviation (σ=0.2), the probability of unseating is calculated for different μs (μ=0.3, 0.4, 0.5). Results are given in Fig. 8a, where the calculated probability of failure is between 10 to 15.0 percent. The second case assumes constant mean μ of 0.4 and standard deviation changing from 0.1 to 0.3 (Fig. 8b). The effect of changing σ is less than that of changing mean μ.

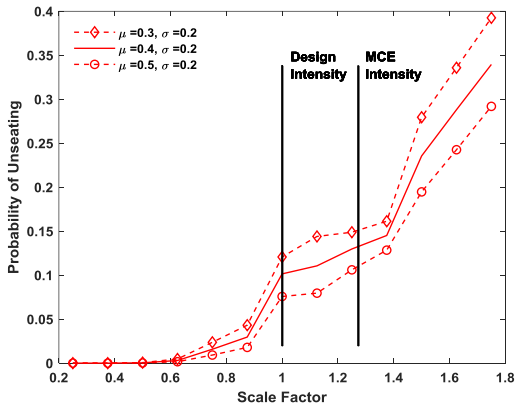

(a)

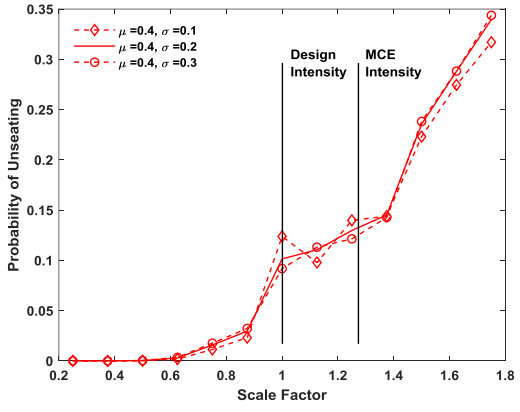

(b)

Fig. 8: Probability of failure for different ground motion intensities and also for different assumptions regarding mean and standard deviation of coefficient of friction, a) constant σ=0.2, b) constant mean μ=0.4

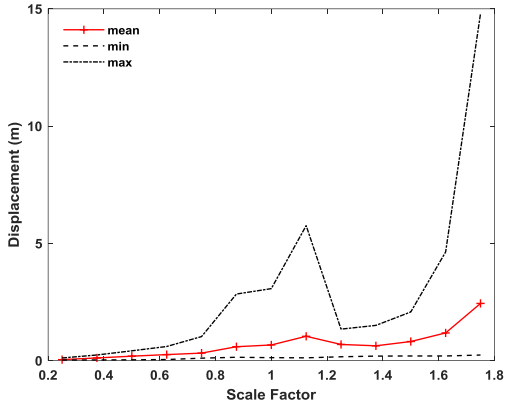

(a)

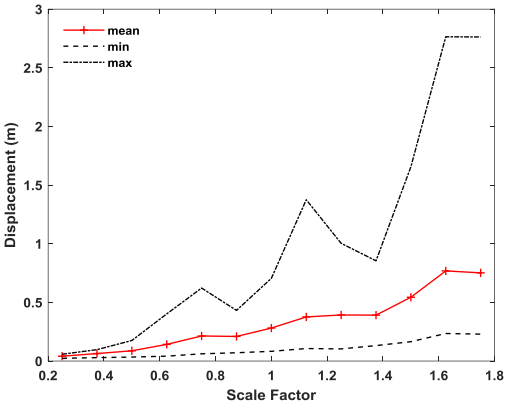

(b)

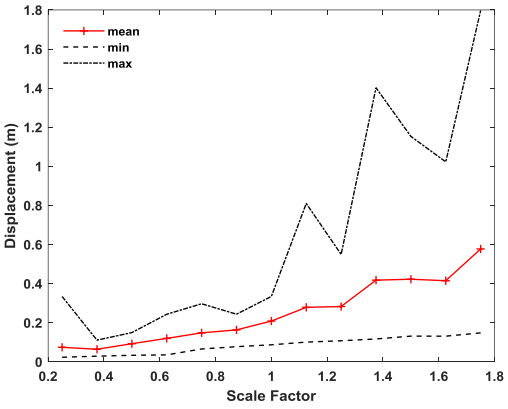

(c)

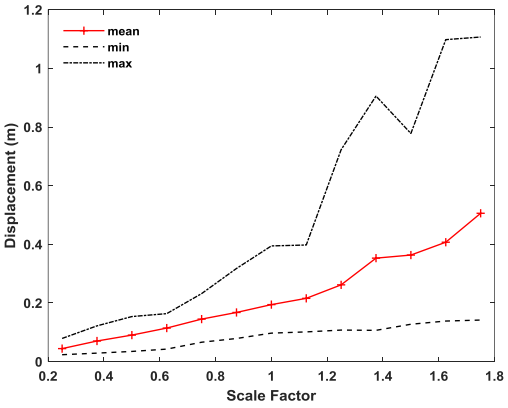

(d)

Fig. 9: Deck displacement in transvers direction, a) μ=0.2, b) μ=0.4, c) μ=0.6, d) μ=0.8

Transverse response

Concentrating on the transverse response, in this section the deck displacement sensitivity to μ and the shear key design strength (V_{sk}) is evaluated. Figure 9 depicts the deck displacement in the transverse direction for four different values of μ. Shear key strength in these analyses is designed for an earthquake with a return period of 100 yrs. The same pattern of behavior observed for longitudinal direction also occurs in the transverse direction. Unrealistic lateral displacement is observed for μ=0.2. The possibility of unseating in the lateral displacement for edge beams, even for μ=0.4 is high.

To investigate the influence of V_{sk} on the lateral displacement of the deck and on the seismic demand imposed on the substructure, analyses are done for different V_{sk}s corresponding to an earthquake return periods of 100 (SLE), 500, 1000 (DBE), and 2500 yrs (MCE). Commonly, strength of shear keys is designed for an earthquake with 1000 yrs return period, that is the design earthquake of AASHTO. All of the following analyses are done assuming μ=0.4.

Figure 10 depicts the impact of shear key design on the column shear and deck displacement, where the onset of slip is depicted in Figure 10a. The response is evaluated adopting different design strengths for the shear key including no shear key, and shear key strength corresponding to SLE, DBE, and MCE. Performance is evaluated for Niigata ground motion scaled to one-quarter of the design intensity (scale factor of 0.25), which simulates a frequent earthquake. Failure of shear keys designed for SLE and DBE is evident in Figures 10b and 10c, where the deck displacement exceeds 50 mm and only the shear key designed for MCE level ground motion survives. This means that even in design for DBE intensity, during frequent ground motions, failure of the shear keys could be imminent. An interesting point is that, after shear key failure, there is no meaningful difference in the displacement of the deck for different schemes of shear key strength that could be attributed to brittle response of shear keys considered in this study. On the other hand, the design of shear keys for MCE, although reduces displacement demand, leads to a significant increase in the column shear force, which is about three times that for the scheme without the shear key.

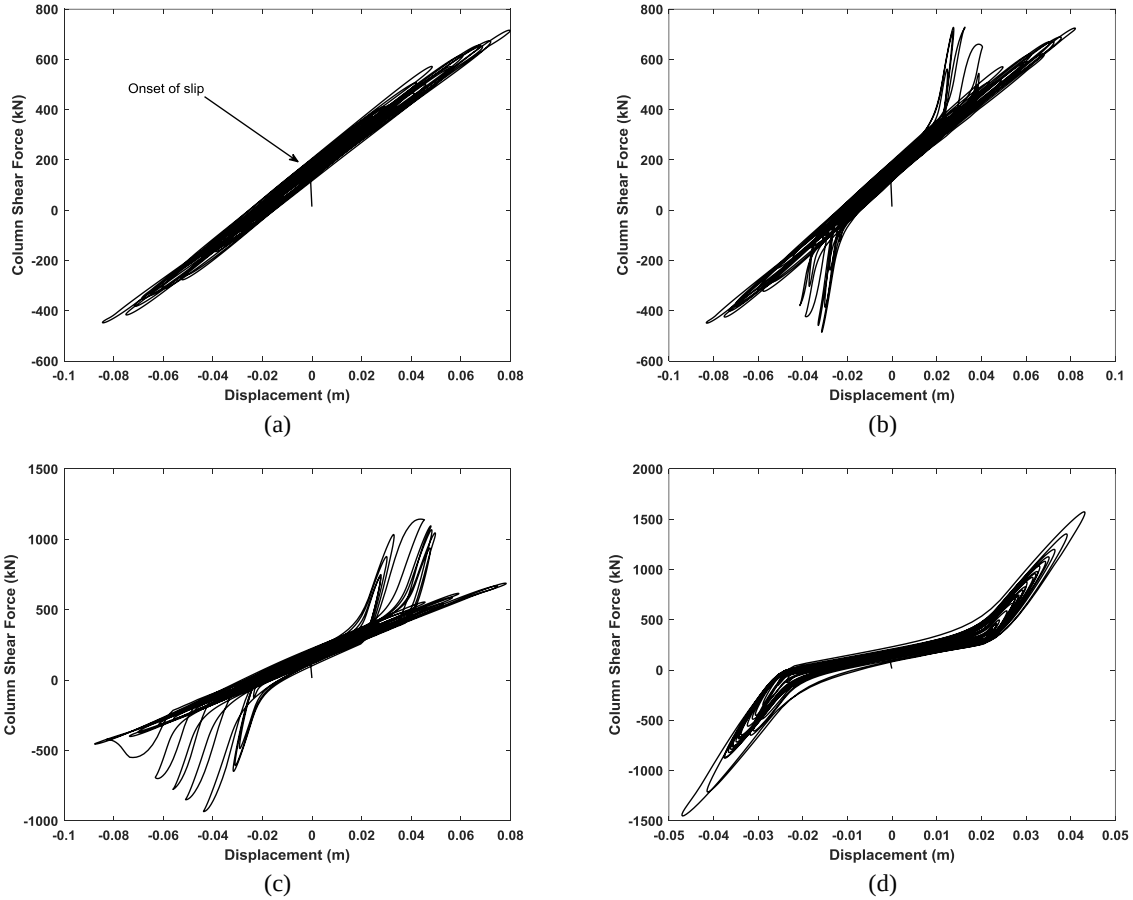

Fig. 10: Column shear force versus deck displacement for bridge subjected to Niigata ground motion with scale factor of 0.25 and for different strength of shear key (μ=0.4), a) no shear key, b) shear key design for SLE, c) shear key design for DBE, d) shear key design for MCE

Returning to the results of IDA, the evolution of mean deck displacement with scale factor is given in Figure 11 for different models corresponding to different design strengths of shear keys. As can be seen, irrespective of the assumed design strength of shear keys, the shear keys fail for seismic hazard corresponding to scale factors larger than 0.6. This figure also shows the inappropriateness of the design of shear keys for SLE, where relatively large lateral displacements could be experienced during earthquakes with small to intermediate intensities. Also shown in this figure are the results for the nonslip model. The inadequacy of the nonslip model in providing a good assessment of the deck displacement is evident in the figure.

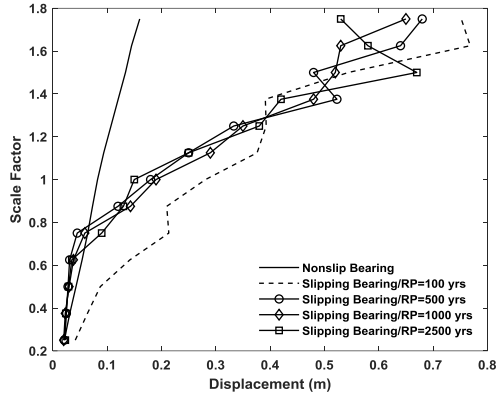

Fig. 11: Evolution of mean deck displacement with scale factors, for different design strength of shear keys of slipping (μ=0.4) and nonslip models.

The results clearly suggest that design strength in the order of earthquake with a return period of 100 yrs could lead to significant slip even at service level ground motions. Also, it could be concluded that the design of the shear key for strength corresponding to earthquakes with return periods larger than 500 yrs, does not provide better protection against the transverse displacement of the deck. This means that design for larger strength does not necessarily avoid shear key failure and there is no justification for designing shear keys for larger return periods. For designs corresponding to return periods larger than 500 yrs, at DBE and MCE levels there is no significant difference between different design schemes, however, the same conclusion could not be extended to the rotational demand in the substructure.

In fact, the design of shear keys for larger strength increases seismic demand on the substructure that is tier 3 of the quasi-isolation system. Figure 12 compares plastic rotations of the columns in different models corresponding to different design strengths of shear keys. This figure shows that using a nonslip model could lead to gross overestimation of the rotational demand. In the case of models accounting for bearing slip, there is a large increase in the rotational demand at a scale factor of 0.5 (approximately corresponding to SLE) for different design schemes which increase steadily for more intense ground motions. For ground motions corresponding to larger scale factors (larger than 0.5) the difference between different design schemes reduces. It is interesting that smaller shear key strengths (e.g., that corresponding to 100 yrs) do not have an appreciable impact on the substructure rotational demand.

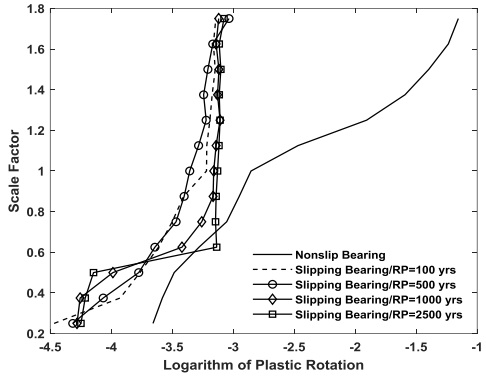

Fig. 12: Evolution of mean columns rotational demand for increasing scale factors, for models accounting for and ignoring bearing slip

6. Conclusion

This paper investigates the seismic performance of three span seat-type bridges with elastomeric bearings on the piers and abutments. The elastomeric bearings do not have endplates, and there is no positive connection between the superstructure and substructure. As reviewed in the paper, different codes/institutes have diverse findings/opinions regarding the coefficient of friction of the bearings (μ) and the design strength of shear keys (V_{sk}) that should be used in the seismic design of bridges. This paper investigates how variation in μ and V_{sk} could affect the seismic performance of seat-type bridges. It is shown that variation of μ results in a significant change in the deck displacement. For the μ values as proposed by some codes (Chinese code for seismic design of highways and AASHTO), i.e., μ=0.15~0.20, there is a significant probability of unseating in the longitudinal and transverse directions. Results also show that tuning V_{sk} for earthquakes with return periods greater than 500 yrs. will not only provide protection against unseating in the transverse direction, but could also increase rotational demand in the substructure. On the other hand, weaker shear keys could lead to substantial slip even during small to medium intensity ground shaking. The results show how a change in these design parameters could affect the seismic assessment of the seat-type bridges. Also, it is shown that using nonslip models in the seismic assessment of these types of bridges could be misleading in the evaluation of the unseating risk and also estimation of plastic demand on the substructures.

References

[1] McDonald, J., Heymsfield, E., and Avent, R. R. (1999), Investigation of elastomeric bearing pad failures in Louisiana bridges, Department of Civil and Environmental Engineering, Louisiana State University.

[2] FHWA (2006), Seismic Retrofitting Manual for Highway Structures : Part 1 – Bridges, Federal Highway Administration, doi: 10.1016/S0140-6736(05)73946-5.

[3] Kelly, J. M. and Konstantinidis, D., (2009), Effect of Friction on Unbonded Elastomeric Bearings, Journal of Engineering Mechanics, 135(9), doi: 10.1061/(asce)em.1943-7889.0000019.

[4] Steelman, J.S., Fahnestock, L.A., LaFave, J.M., Hajjar, J.F., Filipov, E.T., and Foutch, D.A., (2011), Seismic response of bearings for quasi-isolated bridges- Testing and component modeling, Proceedings of the 2011 Structures Congress, doi: 10.1061/41171(401)16.

[5] Filipov, E.T., Fahnestock, L.A., Steelman, J., Hajjar, J.F., LaFave, J.M., and Foutch, D.A., (2013), Evaluation of quasi-isolated seismic bridge behavior using nonlinear bearing models, Engineering Structures, doi: 10.1016/j.engstruct.2012.10.011.

[6] LaFave, J.M., Fahnestock, L., Foutch, D., Steelman, J., Revell, J., Filipov, E., Hajjar, J., (2013), Seismic Performance of Quasi-Isolated Highway Bridges in Illinois, Civil Engineering Studies Illinois Center for Transportation.

[7] IDOT, (2012), Bridge Manual, Illinois Depeartment of Transportation.

[8] Maghsoudi-Barmi, A., Khaloo, A.R., (2020), Experimental investigation of life-time performance of unbounded natural rubber bearings as an isolation system in bridges, Structure and Infrastructure Engineering, doi: 10.1080/15732479.2020.1793208.

[9] Maghsoudi-Barmi, A., Khansefid, A., Khaloo, A.R., Ehteshami, M., (2021), Seismic risk assessment of optimally designed highway bridge isolated by ordinary unbounded elastomeric bearings, Numerical Methods in Civil Engineering, 6(1).

[10] Schrage, I., (1981), Anchoring of bearings by friction, in Joint sealing and bearing systems for concrete structures, world congress on joints and bearings. American Concrete Institute Niagara Falls, NY, USA.

[11] Konstantinidis, D., Kelly, J.M. and Makris, N., (2009), Experimental investigation on the seismic response of bridge bearings, International Conference on Advances in Experimental Structural Engineering.

[12] Filipov, E.T., Hajjar, J.F., Steelman, J.S., Fahnestock, L.A., LaFave, J.M., Foutch, D.A., (2011), Computational analyses of quasi-isolated bridges with fusing bearing components, Proceedings of the 2011 Structures Congress, doi: 10.1061/41171(401)25.

[13] Huang, Q., Liu, H., and Ding, Z., (2019), Dynamical response of the shaft-bearing system of marine propeller shaft with velocity-dependent friction, Ocean Engineering, doi: 10.1016/j.oceaneng.2019.106399.

[14] AASHTO/NSBA, (2004), Steel bridge bearing design and detailing guidelines, AASHTO/NSBA Steel Bridge Collaboration, Washington, D.C.

[15] AASHTO (2017) AASHTO LRFD Bridge Design Specifications, American Association of State Highway and Transportation Officials. Washington, D.C.

[16] AASHTO, (2011), Guide Specifications for LRFD Seismic Bridge Design, 2nd Edition, American Association of State Highway and Transportation Officials, Washington, D.C., doi: 10.1007/s00034-014-9866-6.

[17] Caltrans, (2019), Seismic Design Criteria Version 2.0, California Department of Transportation: Sacramento, CA, U.S.

[18] Huang, W., Xiuli Xu, X., Wang, K., (2018), Numerical Simulation of Steel-Laminated Bearing Considering Friction Slipping, International Journal of Engineering and Technology, 10(2).

[19] Wang, J., Wang, G.F., Yuan, W.K., (2018), The statistical characteristics of static friction, International Journal of Applied Mechanics, doi/10.1142/S1758825118500874.

[20] Chang, W-R., Chang, C-C, Mat, S., and Lesch, M.F., (2008), A methodology to quantify the stochastic distribution of friction coefficient required for level walking, Applied Ergonomics, 39(6). doi: 10.1016/j.apergo.2007.11.003.

[21] Omrani, R., Mobasher, B., Liang, Xiao, and Taciroglu, E., (2015), Guidelines for nonlinear seismic analysis of ordinary bridges: Version 2.0', Caltrans Final Report No. 15-65A0454, doi: 10.13140/RG.2.1.4946.6648.

[22] Kawashima, K., Takahashi, Y., Ge, H., Wu, Z., and Zhang, J., (2009), Reconnaissance report on damage of bridges in 2008 Wenchuan, China, earthquake, Journal of Earthquake Engineering, doi: 10.1080/13632460902859169.

[23] Song, S., Liu, J., and Qian, Y., (2018), Dependence analysis on the seismic demands of typical components of a concrete continuous girder bridge with the copula technique, Advances in Structural Engineering, doi: 10.1177/1369433218757234.

[24] Moinfar, A.A., and Naderzadeh, A., (1990), An immediate and preliminary report on the Manjil, Iran earthquake of 20 june 1990, Bulletin of the New Zealand Society for Earthquake Engineering, doi: 10.5459/bnzsee.23.4.254-283.

[25] Eshghi, S., and Ahari, M.N., (2005), Performance of transportation systems in the 2003 Bam, Iran, earthquake, Earthquake Spectra, doi: 10.1193/1.2098891.

[26] Publication No. 463, (2008), Iranian code for seismic design of bridges.

[27] McKenna, F., (2011), OpenSees: A framework for earthquake engineering simulation, Computing in Science and Engineering, doi: 10.1109/MCSE.2011.66.

[28] Rajesh, B., Dhakal, P., and Maekawa, K., (1999), Modeling for Post-Yield Buckling of Reinforcement, Journal of Structural Engineering, doi: 10.1061/(ASCE)0733-9445(2002)128:9(1139).

[29] Mander, J.B., and Rodgers, G.W., (2015), Analysis of low cycle fatigue effects on structures due to the 2010-2011 Canterbury earthquake sequence, Proceedings of the Tenth Pacific Conference on Earthquake Engineering. Sydney.

[30] Kashani, M.M., Lowes, L.N., Crewe, A.J., Alexander, N.A., (2016), Nonlinear fibre element modelling of RC bridge piers considering inelastic buckling of reinforcement, Engineering Structures, doi: 10.1016/j.engstruct.2016.02.051.

[31] Mander, J.B., Priestley, M.J., and Park, R., (1988), Theoretical stress-strain model for confined concrete, Journal of Structural Engineering, doi: 10.1061/(ASCE)0733-9445(1988)114:8(1804).

[32] Kottari, A., (2016), Horizontal Load Resisting Mechanisms of External Shear Keys in Bridge Abutments, https://escholarship.org/uc/item/0xp4r2hb.

[33] Muthukumar, S., and DesRoches, R., (2006), A Hertz contact model with non-linear damping for pounding simulation, Earthquake Engineering and Structural Dynamics, doi: 10.1002/eqe.557.